CRinc

The University of Kansas Center for Research, Inc.

2291 Irving Hill Drive-Campus West   Lawrence, Kansas 66045

STUDY ON USING A DIGITAL RIDE QUALITY

AUGMENTATION SYSTEM TO TRIM AN ENGINE-OUT

IN A CESSNA 402B

KU-FRL-6132-3

by: Kent E. Donaldson

Supervised by: Dr. Jan Roskam

THE UNIVERSITY OF KANSAS CENTER FOR RESEARCH, INC.
Flight Research Laboratory
Lawrence, Kansas

STUDY ON USING A DIGITAL RIDE QUALITY AUGMENTATION
SYSTEM TO TRIM AN ENGINE-OUT IN A CESSNA 402B

ABSTRACT

A linear model of the Cessna 402B was used to
determine if the control power available to a Ride
Quality Augmentation System was adequate to trim an
engine-out. Two simulations were completed: one using a
steady-state model, and the other using a state matrix
model. The amount of rudder available was not
sufficient in all cases to completely trim the airplane,
but it was enough to give the pilot valuable reaction
time. The system would be an added measure of safety
for only a relatively small amount of development.

TABLE OF CONTENTS

LIST OF FIGURES

LIST OF TABLES

LIST OF ABBREVIATIONS AND SYMBOLS

ABBREVIATIONS

FC1   Flight Condition #1

ICAD   Interactive Control Augmentation Design

RQAS   Ride Quality Augmentation System

SYMBOLS

A   Continuous State Matrix

b   Wing Span, ft

B   Continuous Control Matrix

C_{l_β} Variation of Rolling Moment Coefficient with Sideslip Angle, rad^{-1}

$C_{l_{\delta_{DF}}}$ Variation of Rolling Moment Coefficient with Differential Flap Deflection, rad^{-1}

$C_{l_{\delta_R}}$ Variation of Rolling Moment Coefficient with Rudder Deflection, rad^{-1}

C_{n_β} Variation of Yawing Moment Coefficient with Sideslip Angle, rad^{-1}

$C_{n_{\delta_{DF}}}$ Variation of Yawing Moment Coefficient with Differential Flap Deflection, rad^{-1}

$C_{n_{\delta_R}}$ Variation of Yawing Moment Coefficient with Rudder Deflection, rad^{-1}

C_{y_β} Variation of Side Force Coefficient with Sideslip Angle, rad^{-1}

$C_{y_{\delta_{DF}}}$ Variation of Side Force Coefficient with Differential Flap Deflection, rad^{-1}

$C_{y_{\delta_R}}$ Variation of Side Force Coefficient with Rudder Deflection, rad^{-1}

F_{y_T} Side Force due to Asymmetric Thrust, lb

g Acceleration of Gravity, ft/sec^2

L_T Rolling Moment due to Asymmetric Thrust, ft lbs

m Airplane Mass, slugs

N_T Yawing Moment due to Asymmetric Thrust, ft lbs

ΔN_D Yawing Moment due to Drag of Inoperative Engine, ft lbs

p Perturbed Roll Rate, rad/sec

q Dynamic Pressure, lb/ft^2

r Perturbed Yaw Rate, rad/sec

S Reference (Wing) Area, ft^2

u Control Vector

V_{MC} Minimum Control Speed, ft/sec^2

V_S Stall Speed, ft/sec^2

x State Vector

GREEK SYMBOLS

β Sideslip Angle, deg, rad

γ Glide Path Angle, deg, rad

δ_{DF} Differential Flap Deflection, deg, rad

δ_R Rudder Deflection, deg, rad

ϕ Bank Angle, deg, rad

1. INTRODUCTION

Due to the large increase in the commuter airline industry, with the federal deregulation of major carriers in 1978, more people are riding in small, short-haul, propeller-driven aircraft. This has caused an increased effort to make riding in such an aircraft as pleasant as possible. One project undertaken has been the development of a Ride Quality Augmentation System (RQAS). This system uses acceleration feedback to lessen the effects of turbulence by counteracting the undesirable accelerations with appropriate separate surface control deflections.

It was felt by the developers of this system that since the control power was available, it would also be beneficial to use this system to trim the airplane in the event of an engine-out. This was the basis for the following investigation into using a RQAS to control a Cessna 402B in an engine-out flight condition. The investigation was conducted as part of NASA grant NAG1-345. Mr. Lou Williams is the grant monitor.

Chapter 2 of this report describes the proposed RQAS for the Cessna 402B. The models used to evaluate the system in an engine-out are then given: the steady-state model in Chapter 3 and the small perturbation

1

model in Chapter 4.   The results of using these models
for an engine-out are then discussed in Chapter 5.

2. RIDE QUALITY AUGMENTATION SYSTEM

Reference 1 documents the proposed control surface
modifications for the RQAS in the Lateral-Directional
mode (see Figure 1):

1. Replace the outboard section of the split flap
with a differentially deflecting plain flap that
can deflect +15 to -45 degrees.

2. Use the entire existing rudder (limiting the
RQAS range of deflections to ±5 degrees).

The outboard flaps were computed to have 67% of the
control power of the ailerons in the nonlinear model.

Table 1 summarizes the control surface and actuator
requirements for the RQAS of reference 1.

3. LINEAR STEADY-STATE MODEL

A nonlinear simulation model of the Cessna 402B
(Ref. 2) was used to obtain a linear model about its
most critical condition for an engine out.   That is:

1. sea level;

2. flaps down;

3. full throttle;

4. maximum landing weight.

2
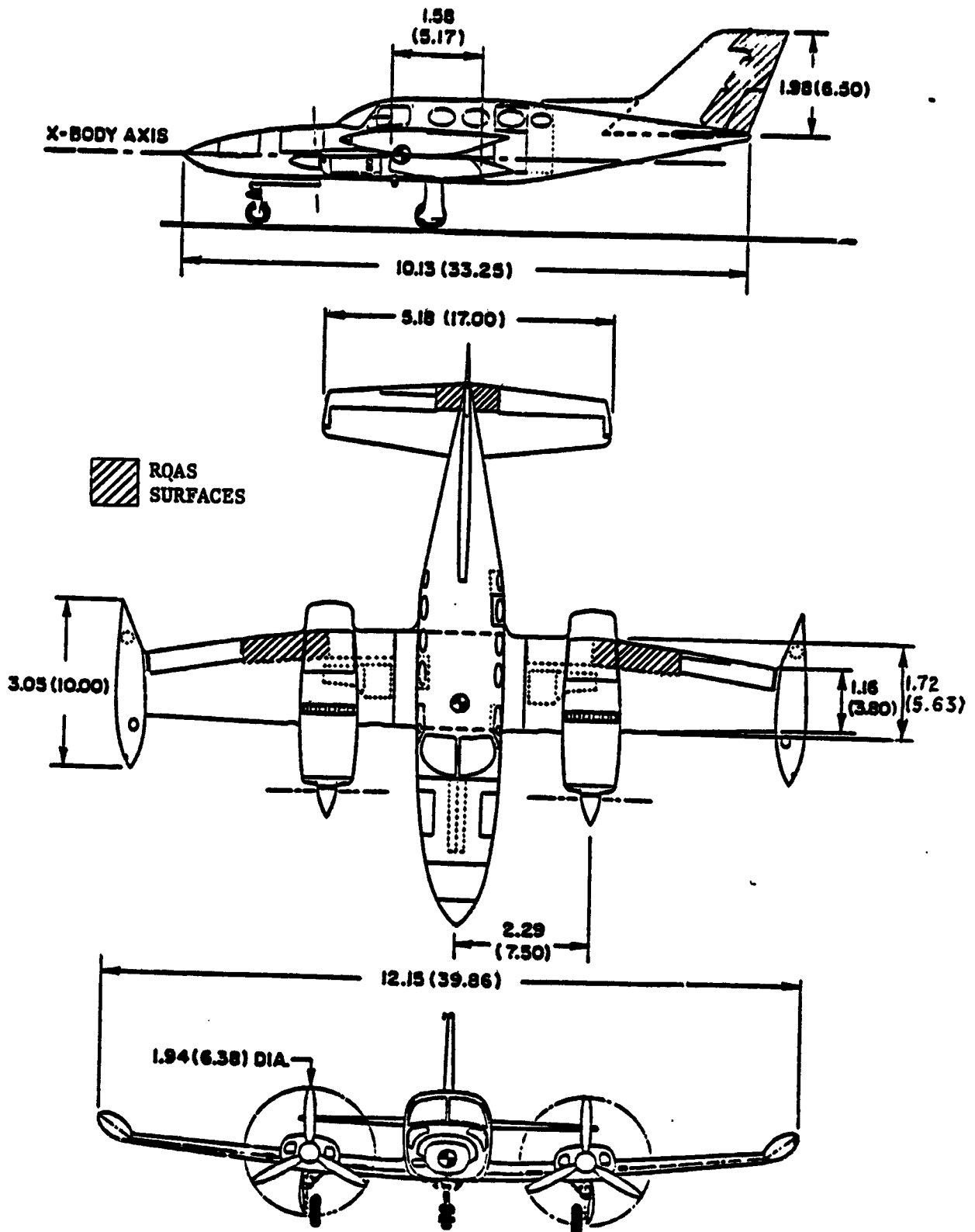
FIGURE 1   Cessna 402B Three-view

**Table 1   Control Surface and Actuator
Requirements**

Control Surface Deflection and Rate Limits

Surface	Deflection Range(deg)	Maximum Rate(deg/sec)
SS Elevator	±5	50
Flap(inboard)	+15 to -45	120
Differential Flap	+15 to -45	120
Rudder[1]	±32	50

Actuator Requirements

Surface	Max Load (lbs)	Speeed (in/sec)	Stroke (in)
SS Elevator	65	3.50	0.75
Flap(inboard)	750	8.50	4.25
Differential Flap	380	8.50	4.25
Rudder	520	3.50	4.50

[1] The deflection is for the standard rudder.   The RQAS
uses a deflection range of ±5 degrees.

This will be called Flight Condition #1 (FC1) and is defined as:

One Engine Out   V = 130 fps   .. = 0 ft

Full Throttle $\bar{x}_{cg}$ = 0.25   W = 6200 lbs

Full Flaps

The stability and control derivatives given in Appendix A, Table A.1 are for the maximum landing weight. Because the maximum landing weight differs from the maximum takeoff weight by less than 2%, the given values were used without correction. Flight condition #1 would be the condition in an emergency go-around.

3.1 STEADY-STATE EQUATIONS

The basic assumption made to determine needed control surface deflection was that the airplane motion could be modelled about a steady-state point as a set of first-order differential equations, as shown in Eqn. 2.1 for an engine-out flight condition.

$$\begin{bmatrix} C_{y_\beta} & C_{y_{\delta_{DF}}} & C_{y_{\delta_R}} \\ C_{l_\beta} & C_{l_{\delta_{DF}}} & C_{l_{\delta_R}} \\ C_{n_\beta} & C_{n_{\delta_{DF}}} & C_{n_{\delta_R}} \end{bmatrix} \begin{Bmatrix} \beta \\ \delta_{DF} \\ \delta_R \end{Bmatrix} = \begin{Bmatrix} \dfrac{-(mg\sin\phi\cos\gamma + F_{Y_T})}{qS} \\ \dfrac{-L_T}{qSb} \\ \dfrac{-(N_T + \Delta N_D)}{qSb} \end{Bmatrix} \quad (2.1)$$

These equations have been uncoupled from the full 6 degree of freedom equations by choosing bank angle, ϕ. They are written in the stability axis system (see

section 3.2). Their derivation can be found in
reference 3.

3.2 COORDINATE REFERENCE SYSTEM

The body-axis system is an orthogonal, right-hand
set of axes with its origin at the airplane's center of
mass. The X-axis lies along the centerline of the body.
The X- and Z-axes lie in the airplane plane of symmetry,
while the Y-axis is pointed out the right wing of the
airplane. This can be seen in Figure 2.

The non-dimensional derivatives listed in Appendix
A, Table A.1 are given in the stability-axis system.
This system is also an orthogonal, right-hand set of
axes with its origin at the center of mass of the
airplane. The difference between the body- and the
stability-axis systems is that the stability X-axis is
oriented in the direction of the steady-state velocity
of the airplane on its XZ-plane. They both share the
same Y-axis as seen in Figure 2.

3.3 DEVELOPMENT

The thrust was calculated using an engine model and
its average propeller efficiency. The average propeller
efficiency is greater than the actual propeller
efficiency by approximately 6%; therefore, the actual
pitching moment and yawing moment during engine-out
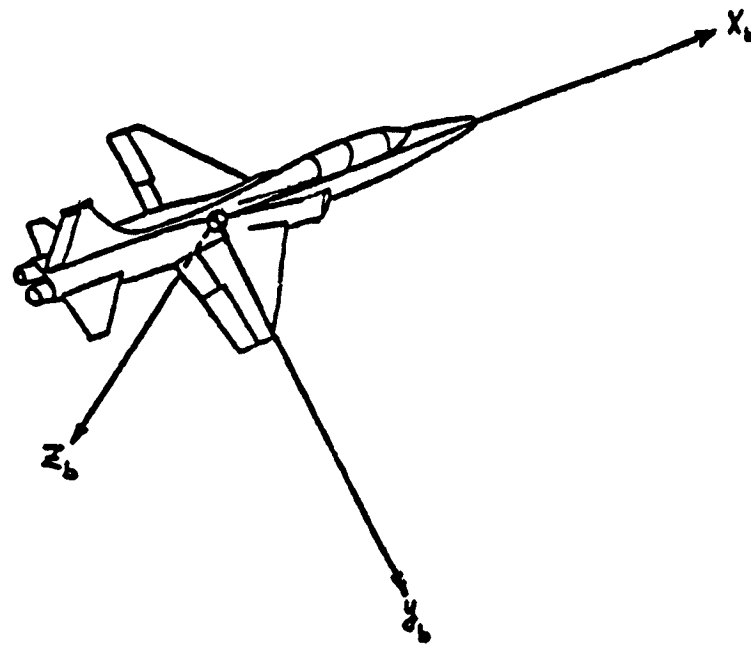
Body Axis Coordinate System
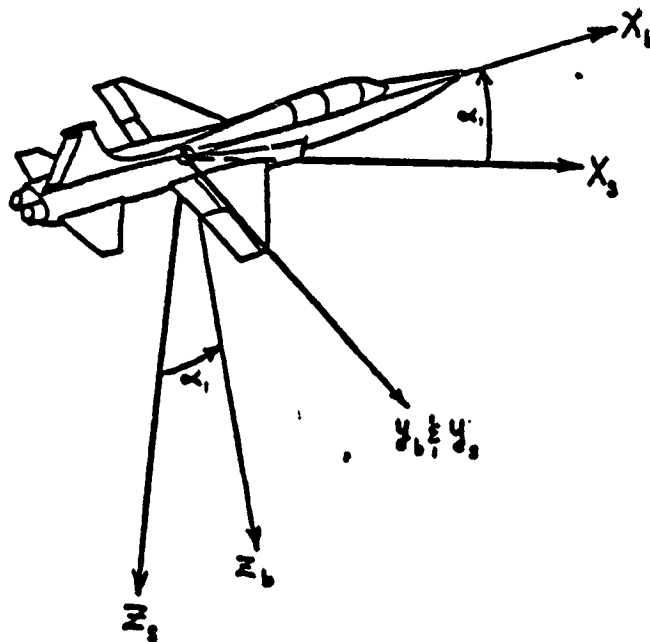
Stability Axis Coordinate System

FIGURE 2   Airplane Coordinate Systems

would be slightly less. The propeller efficiencies are given in Appendix A.

By assuming a weight and flight condition, the angle of attack was obtained from the airplane lift-curve slope and intercept as shown in Appendix A. Some of the derivatives are functions of angle of attack. Once the angle of attack was calculated, the non-dimensional derivatives were obtained from reference 2. They are given in Appendix A.

By varying the speed and the vertical tail size and solving Equation 2.1 as shown in Appendix A, the sideslip, rudder, and differential flap deflections were determined. Figure 3 shows how rudder deflection varies with flight condition.

3.4 RESULTS

It can be seen from Figure 3 that at speeds below approximately 125 fps, there is not enough rudder to keep the airplane in straight-line flight. This is the minimum control speed, V_{MC}. This is 15 fps less than the minimum control speed given in the operating handbook; therefore, a minimum control speed of 130 fps is still conservative. At 130 fps, it was found that to fly straight with a bank angle, ϕ, of -5° required 30° of rudder deflection, 7.5° of differential flap deflection, with a sideslip of -3°. The pedal force

8

The chart shows "RUDDER REQUIRED, δ_R (deg)" on the vertical axis versus "SPEED, V (fps)" on the horizontal axis.

Annotations on the chart:

CESSNA 402B (BASIC)
W = 6300 lb $\bar{X}_{c.g.}$ = 0.25
ϕ = -5° FLAPS DOWN
SEA LEVEL
FULL THROTTLE
ONE ENGINE OUT

V_S V_{MC} $1.2 V_S$

MAX. RUDDER DEFLECTION

FACTOR TIMES
EXISTING V.T. SIZE
0.50
0.75
1.00
1.25

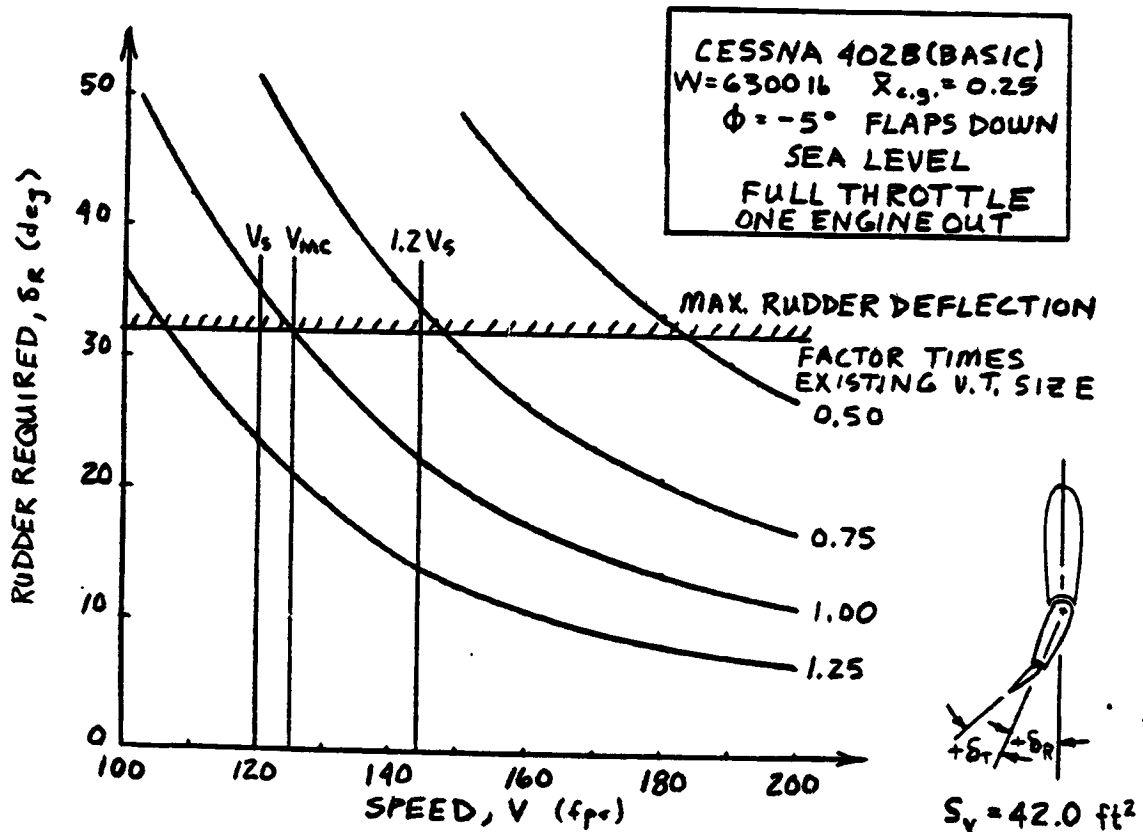$+\delta_T$ $+\delta_R$

S_v = 42.0 ft²

FIGURE 3   Rudder required for an engine-out
on a Cessna 402B

9

required was also found to be within federal
regulations.

It can also be seen from Figure 3 that if one-
fourth of the vertical tail were removed, the airplane
would no longer meet FAR 23 requirements. FAR 23
requires that the minimum control speed, V_{MC} be greater
than $1.2V_S$. This model does not account for any
transient phenomena of the airplane in reaching its
steady-state condition.

4. SMALL PERTURBATION MODEL

The non-linear simulation model was also used to
develop a linear model to study the dynamic behavior of
the Cessna 402B in open- and closed-loop simulations.
This was only done for FC1.

4.1 EQUATIONS OF MOTION

From the assumptions made in the steady-state
model, a new set of matrix equations can be written:

$$\dot{x} = A x + B u \tag{3.1}$$

where

$$x' = \{\beta, p, r, \phi\}, \text{ and}$$
$$u' = \{\delta_{DF}, \delta_R\}.$$

Derivations of this equation can be found in
reference 4. These matrices are defined in Appendix A.
The matrices used for FC1 are given in Table 2.

Table 2 Small Perturbation Matrices

Cessna 402B (FC1)

$$
A = \begin{bmatrix}
-0.105 & -0.000867 & -0.9899 & 0.245 \\
-1.329 & -1.752 & 0.483 & 0.0 \\
1.408 & -0.0428 & -0.299 & 0.0 \\
0.0 & 1.0 & 0.149 & 0.0
\end{bmatrix}
$$

$$
B = \begin{bmatrix}
0.0 & 0.0306 \\
-0.968 & 0.206 \\
0.0603 & -0.835 \\
0.0 & 0.0
\end{bmatrix}
$$

$$
D = \begin{bmatrix}
0.0 \\
-0.0468 \\
0.445 \\
0.0
\end{bmatrix}
$$

Equation 3.1 is written with the following assumptions:

    1. perturbations are small, and

    2. initial condition is a straight-line

    trimmed flight condition.

4.2 COORDINATE REFERENCE SYSTEM

All of the dimensional and non-dimensional derivatives were calculated in the stability-axis system of Figure 2. The instruments onboard the airplane will sense the body-axis motion. This can be simply transformed to the stability-axis by rotating about the Y-axis by the airplane angle of attack.

4.3 DEVELOPMENT

To simulate an engine-out situation using the state matrices, a disturbance matrix, D, was added to the state and control matrices in Equation 3.1 yielding Equation 3.2. This disturbance matrix was made up of the constant angular accelerations imparted on the airplane in the pitch and yaw directions due to the engine-out. In all the cases, this matrix was commanded to "turn on" at one second into the simulation.

$$\dot{x} = A\,x + B\,u + D\,w \qquad\qquad (3.2)$$

where

$$w = \{0 \text{ or } 1\}$$

The open-loop response of the airplane with the addition of the disturbance matrix was calculated using

12

the Interactive Control Augmentation Design program (ICAD)[5]. This was done on the University of Kansas School of Engineering's Harris computer system. The closed-loop response was also done on ICAD.

As allowed by FAR 23, a bank angle of -5° was used to lower the rudder required as much as possible. This turned out to be a difficult task on ICAD as currently written. Ideally, bank angle, sideslip, and yaw rate should be driven to -5°, 0, and 0 simultaneously. To get these, only bank angle was commanded and all the variables except roll rate were weighted heavily. This gave large transient values for control positions and rates, but in an actual system this would not happen. Figure 4 shows an example time history. The average values of control deflections and control rates have been drawn to show an approximation of what would actually happen.

It can be seen that to trim the airplane requires all 32° of the rudder to be available to the RQAS. As proposed, only 5° of rudder deflection is available to the RQAS; therefore, time histories were also simulated allowing only 5 and 15 degrees of rudder deflection. With 15° of rudder, the RQAS would be able to trim an engine out at speeds above about 170 fps. Five degrees
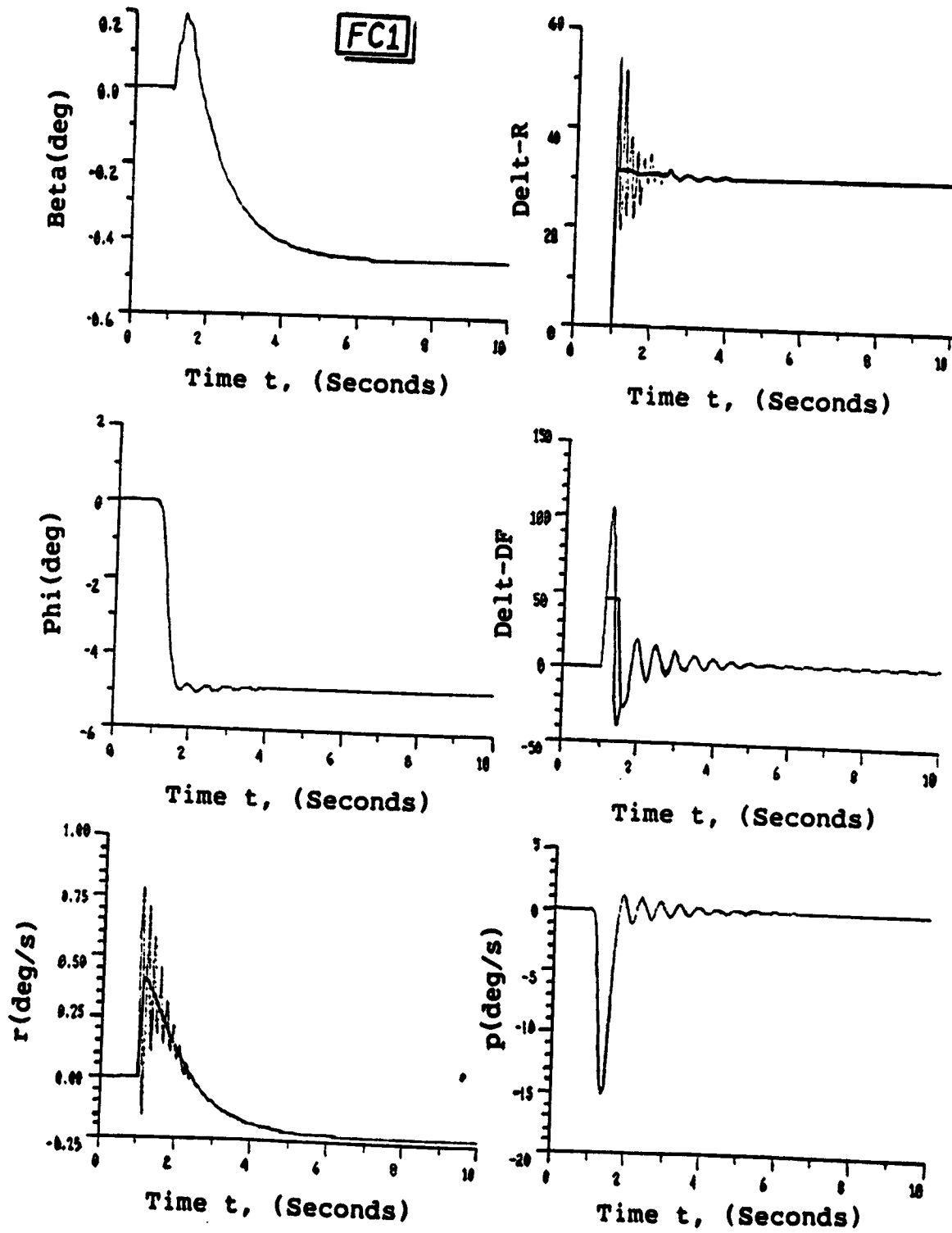
FIGURE 4 Time history of an engine-out in a RQAS controlled Cessna 402B

14

only slows the rates and could not trim the airplane below its "never exceed" speed.

5. DISCUSSION OF RESULTS

The control deflections obtained for FC1 were:

Model	β (deg)	δ_R (deg)	δ_{DF} (deg)
Steady-State	-2.9	30.4	7.5
Small Perturbation	-5.0	30.0	5.0

These values were obtained for a steady-state velocity of 130 fps. The difference in the values between the two models is due to the fact that in the small perturbation model, yaw and pitch rate are not exactly zero. The bank angle is also not quite -5°. It can also be noted from Figure 4 that the RQAS has the airplane trimmed in a fraction of a second, much faster than a human pilot could react. This result is obtained assuming the servo is modelled as a first-order lag.

The slowing of the yaw rate due to only 5° of rudder deflection would give the pilot valuable time to react to the increasing sideslip. In addition, the differential flaps have far more control power than is needed to control roll and bank angle. The quicker the airplane reaches a bank angle of -5°, the longer the pilot has to respond to the yaw.

15

The RQAS has two obvious advantages. First, if the dynamic pressure is high enough and the available rudder is adequate, the RQAS could control an engine-out without the pilot touching the controls. Second, the RQAS would give the pilot more time to react to the engine-out even if the RQAS was not able to trim the airplane entirely.

In addition, the RQAS will introduce digital computers into commuter airplanes which could then be used for many other jobs which of themselves do not warrant the expense of a computer.

If only 5° of rudder deflection is deemed adequate, no modifications need to be made in addition to those proposed for the RQAS. The RQAS block diagram is shown in Figure 5. This system would treat the engine-out as a large disturbance. The gains chosen in the normal use of the RQAS, however, might not be suitable for the engine-out. In that case, engine-out sensors would be required to tell the system when to change gains.

Giving more control power to the system for an engine-out could be done in two ways. First, the RQAS could be given the authority to move the rudder more than 5°. This would require a proportionately stronger actuator, but it would not change the stroke given in Table 1 which is for 32°. Secondly, an engine-out
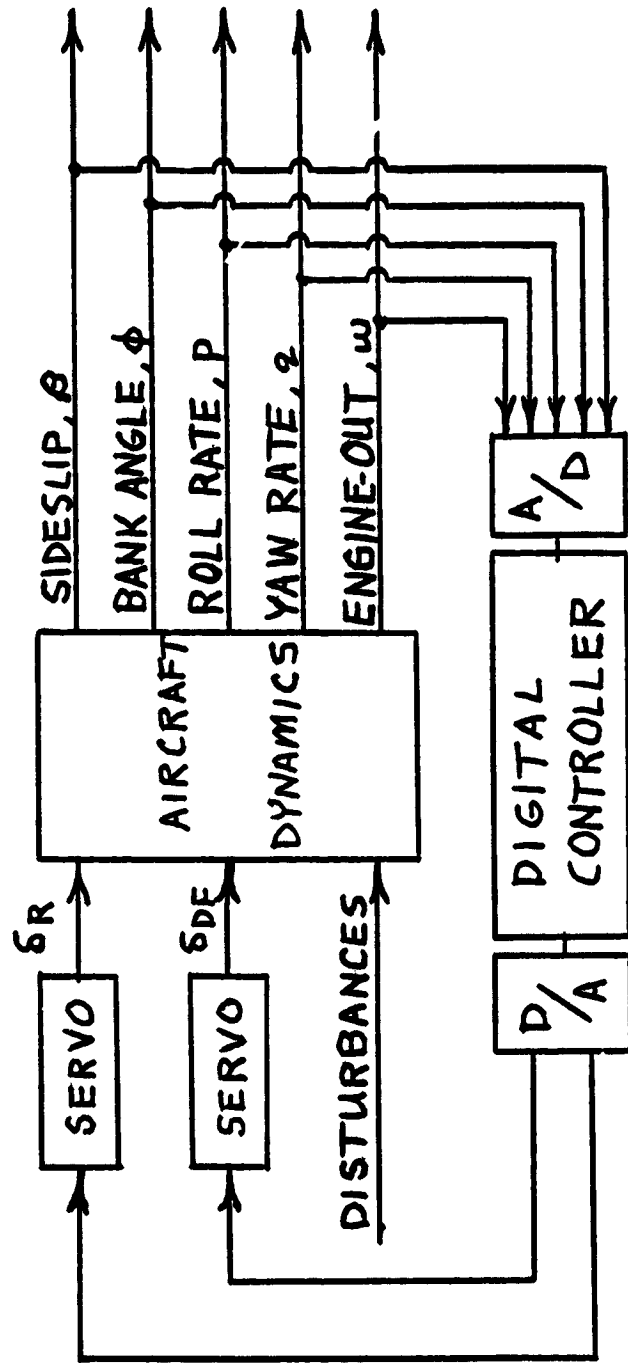
16

FIGURE 5   RQAS Block Diagram

sensor could trigger a change in the amount of rudder allowed so that the RQAS is still only allowed 5° while the engine-out is allowed more.

No additional software will be required if gain scheduling is not needed or is already incorporated in the RQAS. The components needed for this system are a hydraulic pump to be mounted on one of the engines, an accumulator, and a set of electro-hydraulic actuators. The design of the actuator and its implementation will be contracted to Cessna. In addition, a set of engine-out sensors will be required. Reliability, ease of implementation, and cost of these should be investigated.

6. CONCLUSIONS AND RECOMMENDED RESEARCH

6.1 CONCLUSIONS

The following conclusions were reached:

1. The RQAS with control of all 32° of rudder deflection can trim an engine-out in any steady-state flight condition.

2. With only the proposed 5° of rudder deflection, the RQAS can slow the divergence of the airplane significantly.

3. Using only the proposed control surface modifications, implementing the engine-out

capability would require a set of engine-out
sensors and the incorporation of gain scheduling.

4. If it is deemed necessary to use more than the 5
degrees of rudder needed by the RQAS, the actuator
would need to be proportionately stronger.

6.2 RECOMMENDED RESEARCH

Further development of this project must include
the following steps:

1. Perform a preliminary failure analysis for
rudder deflections greater than 5 degrees.

2. Use the gains required at the most
critical condition to see their effect in other
conditions,

3. Examine and evaluate options available to
sense an engine-out,

4. Investigate the possibility of increasing
the amount of rudder deflection available to
the RQAS,

5. Design and build the necessary hardware,

6. Perform a flight test of the system on the
Cessna 402B.

References:

1. Downing, D.R.; Davis, D.J.; Linse, D.J.; Entz, D.P.: "Preliminary Control Law and Hardware Designs For a Ride Quality Augmentation System For Commuter Aircraft", NAG1-345, Feb 1986.

2. Hoh, R.H.; Mitchell, D.G.; Myers, T.T.: "Simulation Model of Cessna 402B". NASA CR 152176, July 1978.

3. Roskam, J.: Airplane Flight Dynamics and Automatic Flight Controls, Part I. Roskam Aviation and Engineering Corp. 1979.

4. Roskam, J.: Airplane Flight Dynamics and Automatic Flight Controls, Part II. Roskam Aviation and Engineering Corp. 1979.

5. Hammond, T.A.; Amin, S.P.; Paduano, J.D.; Downing, D.R.: Design of a Digital Ride Quality Augmentation System For Commuter Aircraft, NASA CR 172419, Oct 1984.

6. Davis, D.J., "A Comparison of Two Optimal Regulator Design Techniques for the Weighting of Output Variables Which are Linear Combinations of States and Controls", M.S. Thesis, The University of Kansas, Lawrence, KS, 1986.

7. Hoak, D.E. et al; USAF Stability and Control DATCOM Wright Patterson Air Force Base, Ohio, 45433, April, 1976.

APPENDIX A   Cessna 402B Stability Derivatives

This appendix gives the method used for estimating the airplane angle of attack and determining its stability and control derivatives.

Because weight, wing area, and dynamic pressure are known, the airplane lift coefficient can be found from the equation:

$$W = C_L \bar{q} S$$

From this lift coefficient, the ΔC_L due to flaps from reference 2 was subtracted. This lift coefficient was then found on Figure A.1 and its corresponding angle of attack was read. The airplane angle of attack was then used to obtain the non-dimensional derivatives from reference 2. These are listed for an angle of attack, α, of 8.5° in Table A.1.

The engine model was taken from reference 2. This gave the maximum power of a C402B engine as 300 brake horsepower. The propeller efficiencies, average and actual, are given in Figure A.2. Thrust was then calculated using the following equation:

$$T = \frac{550 \; BHP}{V} \eta_p \qquad (A.1)$$

where

η_p = Propeller Efficiency

V = Airplane Speed

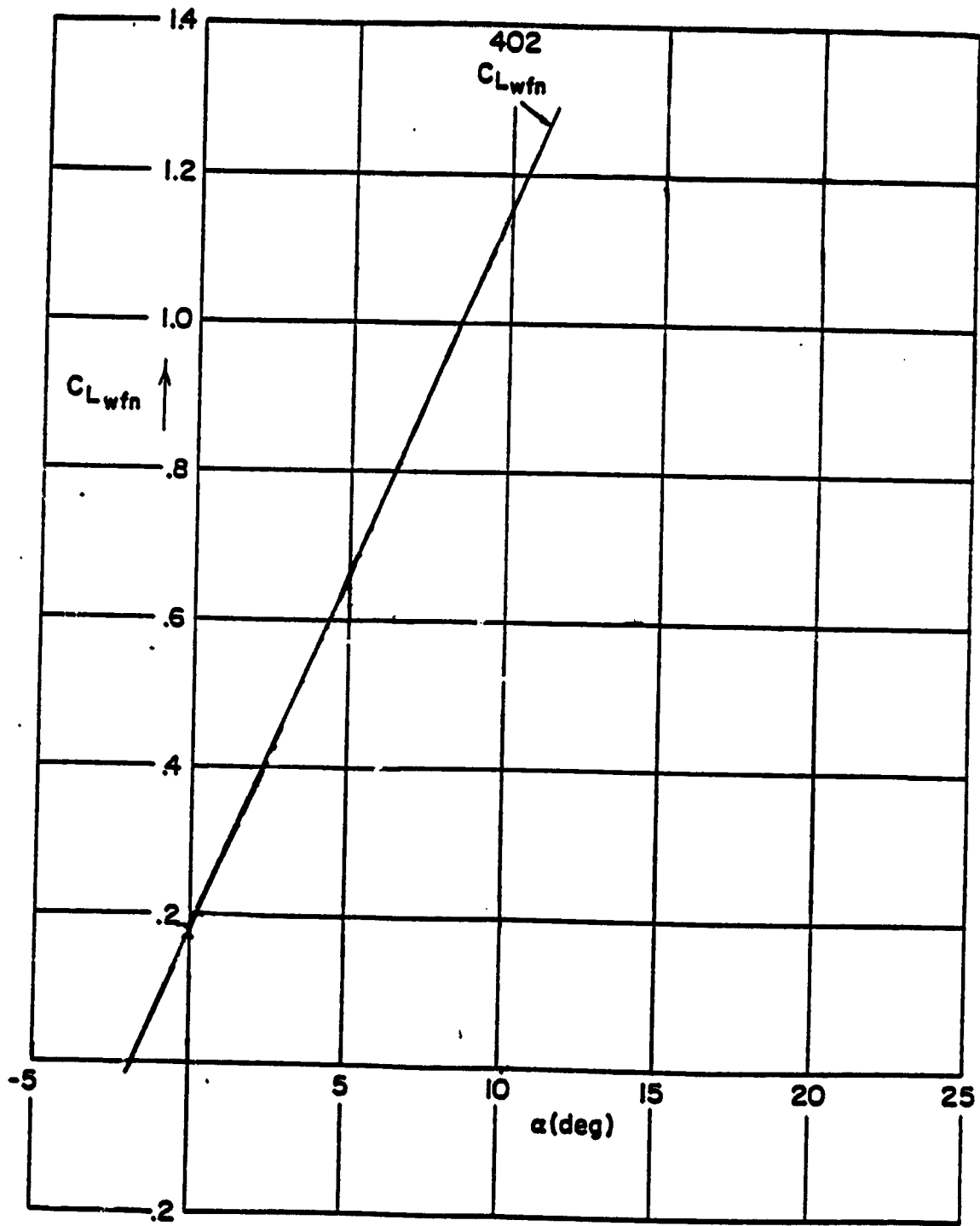BHP = Engine Brake Horsepower

A.1

Figure A.1 Approximate Cessna 402B(Tail-Off) Lift-Curve

A.2

## Table A.1 Lateral-Directional Non-dimensional Stability Derivatives

Cessna 402B

One Engine Out   V = 130 fps   h = 0 ft

Full Throttle $\overline{x}_{cg}$ = 0.25   W = 6200 lbs

Full Flaps

Derivatives

Cy_β = -0.670 rad^{-1} Cy_p = -0.00063

$Cy_{\delta R}$ = 0.195 rad^{-1} Cy_r = 0.42

$Cy_{\delta DF}$ = 0.0 rad^{-1} Cn_p = -0.084

Cn_β = 0.129 rad^{-1} Cn_r = -0.170

$Cn_{\delta R}$ = -0.0795 rad^{-1} Cl_p = -0.81

$Cn_{\delta DF}$ = 0.0057 rad^{-1} Cl_r = 0.216

Cl_β = -0.0888 rad^{-1}

$Cl_{\delta R}$ = 0.0146 rad^{-1}

$Cl_{\delta DF}$ = -0.0685 rad^{-1}
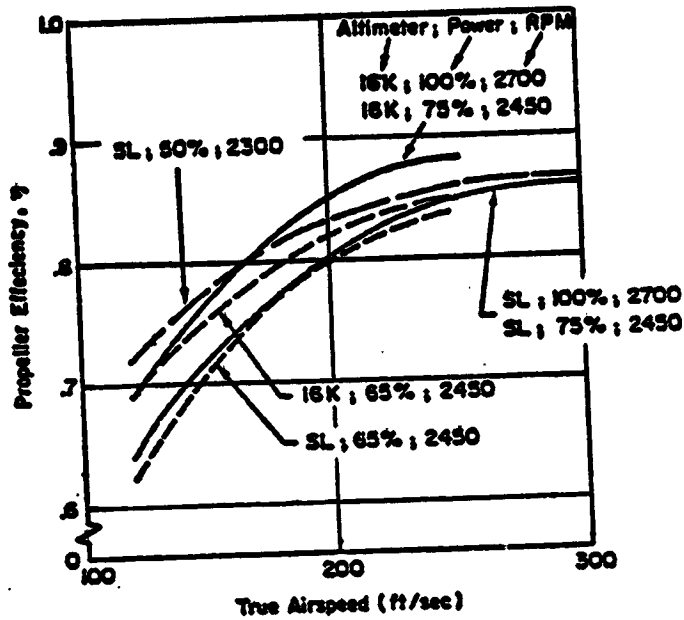
Propeller Efficiency at Several Flight Conditions
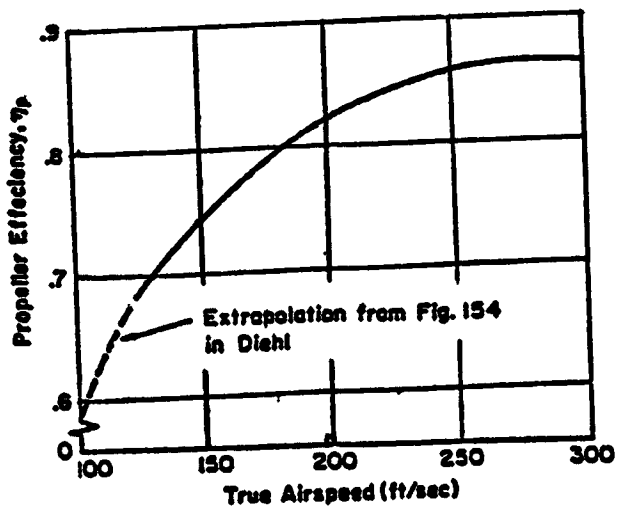
Assumed Average Propeller Efficiency for All Flight Conditions

Figure A.2   Propeller Efficiencies

A.4

From Figure 1, it can be seen that the thrust from one
engine creates a moment about the airplane center of
gravity with a moment arm of 7.50 feet. The orientation
of the thrust line of one of the engines is given in
reference 2. By finding the X and Z components of the
thrust, the moments, N_T and L_T, can be found from:

$$N_T = 7.50 \; T_X, \text{ and}$$

$$L_T = 7.50 \; T_Z.$$

Reference 2 also gives the ΔC_D due to an engine-out.
ΔN_D in Equation 2.1 is the yawing moment due to drag on
the inoperative engine and is:

$$\Delta N_D = 7.50 \; \Delta C_D \; \bar{q} \; S$$

Equation 2.1 was then solved to obtain the sideslip,
differential flap deflection, and rudder deflection
required. To account for changing the vertical tail
size, the non-dimensional derivatives were recalculated
and are summarized in Table A.2.

The dimensional derivatives were then calculated as
shown in Table A.3. These were calculated using:

$$I_{xx} = 11100 \text{ slug ft}^2$$

$$I_{zz} = 14900 \text{ slug ft}^2$$

$$I_{xz} = -583 \text{ slug ft}^2$$

To use these in the state matrices, Table A.4, they must
be in the form shown in Table A.5, where,

$$A_1 = I_{xz}/I_{xx} \quad \text{and} \quad B_1 = I_{xz}/I_{zz} \; .$$

A.5

Table A.2 Variation of Derivatives with Vertical Tail Size

Cessna 402B (FC1)

Relative V.T. Size	C_{n_β} deg^{-1}	$C_{y_{\delta_R}}$ deg^{-1}	$C_{n_{\delta_R}}$ deg^{-1}	$C_{l_{\delta_R}}$ deg^{-1}
0.50	0.00089	0.00165	-0.00070	0.000155
0.75	0.00165	0.00248	-0.00104	0.000230
1.00	0.00240	0.00330	-0.00139	0.000310
1.25	0.00316	0.00413	-0.00174	0.000388

Note: $C_{n_{\beta_{WB}}} = -0.00062$ deg^{-1} was calculated from ref. 7

Table A.3 State Matrices

$$\dot{x} = \begin{bmatrix} \dot{\beta} \\ \dot{p} \\ \dot{r} \\ \dot{\phi} \end{bmatrix}$$

$$A = \begin{bmatrix} Y_\beta' & Y_p' & Y_r' & Y_\phi' \\ L_\beta' & L_p' & L_r' & 0 \\ N_\beta' & N_p' & N_r' & 0 \\ 0 & 1 & \tan\theta_1 & 0 \end{bmatrix} \qquad x = \begin{bmatrix} \beta \\ p \\ r \\ \phi \end{bmatrix}$$

$$B = \begin{bmatrix} Y_{\delta_{df}}' & Y_{\delta_{sr}}' \\ L_{\delta_{df}}' & L_{\delta_{sr}}' \\ N_{\delta_{df}}' & N_{\delta_{sr}}' \\ 0 & 0 \end{bmatrix}, \qquad u = \begin{bmatrix} \delta_{df} \\ \delta_{sr} \end{bmatrix}$$

A.7

Table A.4 Lateral-Directional Dimensional Stability Derivatives [3]

$$Y_\beta = \frac{\bar{q}_1 S C_{y_\beta}}{m} \quad (\text{ft sec}^{-2})$$

$$Y_p = \frac{\bar{q}_1 S b C_{y_p}}{2mU_1} \quad (\text{ft sec}^{-1})$$

$$Y_r = \frac{\bar{q}_1 S b C_{y_r}}{2mU_1} \quad (\text{ft sec}^{-1})$$

$$Y_{\delta_A} = \frac{\bar{q}_1 S C_{y_{\delta_A}}}{m} \quad \begin{array}{l}(\text{ft sec}^{-2} \text{ or} \\ \text{ft sec}^{-2} \text{ deg}^{-1})\end{array}$$

$$Y_{\delta_R} = \frac{\bar{q}_1 S C_{y_{\delta_R}}}{m} \quad \begin{array}{l}(\text{ft sec}^{-2} \text{ or} \\ \text{ft sec}^{-2} \text{ deg}^{-1})\end{array}$$

$$L_\beta = \frac{\bar{q}_1 S b C_{\ell_\beta}}{I_{xx}} \quad (\text{sec}^{-2})$$

$$L_p = \frac{\bar{q}_1 S b^2 C_{\ell_p}}{2I_{xx}U_1} \quad (\text{sec}^{-1})$$

$$L_r = \frac{\bar{q}_1 S b^2 C_{\ell_r}}{2I_{xx}U_1} \quad (\text{sec}^{-1})$$

$$L_{\delta_A} = \frac{\bar{q}_1 S b C_{\ell_{\delta_A}}}{I_{xx}} \quad \begin{array}{l}(\text{sec}^{-2} \text{ or} \\ \text{sec}^{-2} \text{ deg}^{-1})\end{array}$$

$$L_{\delta_R} = \frac{\bar{q}_1 S b C_{\ell_{\delta_R}}}{I_{xx}} \quad \begin{array}{l}(\text{sec}^{-2} \text{ or} \\ \text{sec}^{-2} \text{ deg}^{-1})\end{array}$$

$$N_\beta = \frac{\bar{q}_1 S b C_{n_\beta}}{I_{zz}} \quad (\text{sec}^{-2})$$

$$N_{T_\beta} = \frac{\bar{q}_1 S b C_{n_{T_\beta}}}{I_{zz}} \quad (\text{sec}^{-2})$$

$$N_p = \frac{\bar{q}_1 S b^2 C_{n_p}}{2I_{zz}U_1} \quad (\text{sec}^{-1})$$

$$N_r = \frac{\bar{q}_1 S b^2 C_{n_r}}{2I_{zz}U_1} \quad (\text{sec}^{-1})$$

$$N_{\delta_A} = \frac{\bar{q}_1 S b C_{n_{\delta_A}}}{I_{zz}} \quad \begin{array}{l}(\text{sec}^{-2} \text{ or} \\ \text{sec}^{-2} \text{ deg}^{-1})\end{array}$$

$$N_{\delta_R} = \frac{\bar{q}_1 S b C_{n_{\delta_R}}}{I_{zz}} \quad \begin{array}{l}(\text{sec}^{-2} \text{ or} \\ \text{sec}^{-2} \text{ deg}^{-1})\end{array}$$

Table A.5 Modified Lateral-Directional Dimensional
Stability Derivatives [6]

$Y'_\beta = Y_\beta/U_1$

$Y'_p = Y_p/U_1$

$Y'_r = (Y_r/U_1)-1$

$Y'_\phi = g\cos\theta_1/U_1$

$Y'_{\delta_{df}} = Y_{\delta_{df}}/U_1$

$Y'_{\delta_{sr}} = Y_{\delta_{sr}}/U_1$

$L'_\beta = (A_1N_\beta+L_\beta)/(1-A_1B_1)$

$L'_p = (A_1N_p+L_p)/(1-A_1B_1)$

$L'_r = (A_1N_r+L_r)/(1-A_1B_1)$

$L'_{\delta_{df}} = (A_1N_{\delta_{df}}+L_{\delta_{df}})/(1-A_1B_1)$

$L'_{\delta_{sr}} = (A_1N_{\delta_{sr}}+L_{\delta_{sr}})/(1-A_1B_1)$

$N'_\beta = (B_1L_\beta+N_\beta)/(1-A_1B_1)$

$N'_p = (B_1L_p+N_p)/(1-A_1B_1)$

$N'_r = (B_1L_r+N_r)/(1-A_1B_1)$

$N'_{\delta_{df}} = (B_1L_{\delta_{df}}+N_{\delta_{df}})/(1-A_1B_1)$

$N'_{\delta_{sr}} = (B_1L_{\delta_{sr}}+N_{\delta_{sr}})/(1-A_1B_1)$